frontiers | Frontiers in Marine Science

TYPE Original Research
PUBLISHED 12 August 2022
DOI 10.3389/fmars.2022.960338

OPEN ACCESS

EDITED BY
Clara F. Rodrigues,
University of Aveiro, Portugal

REVIEWED BY
Niels De Winter,
Vrije University Brussel, Belgium
Joachim Reitner,
University of Göttingen, Germany

*CORRESPONDENCE
Dong Feng
dfeng@shou.edu.cn

SPECIALTY SECTION
This article was submitted to Deep-Sea Environments and Ecology, a section of the journal Frontiers in Marine Science

RECEIVED 02 June 2022
ACCEPTED 25 July 2022
PUBLISHED 12 August 2022

CITATION
Wang X, Fan D, Kiel S, Gong S, Liang Q, Tao J, Chen D and Feng D (2022) Archives of short-term fluid flow dynamics and possible influence of human activities at methane seeps: Evidence from high-resolution element geochemistry of chemosynthetic bivalve shells. *Front. Mar. Sci.* 9:960338. doi: 10.3389/fmars.2022.960338

Archives of short-term fluid flow dynamics and possible influence of human activities at methane seeps: Evidence from high-resolution element geochemistry of chemosynthetic bivalve shells

Xudong Wang[1,2], Danling Fan[1], Steffen Kiel[3], Shanggui Gong[1], Qiangyong Liang[4], Jun Tao[4], Duofu Chen[1,2] and Dong Feng[1,2]*

[1]Shanghai Engineering Research Center of Hadal Science and Technology, College of Marine Sciences, Shanghai Ocean University, Shanghai, China, [2]Laboratory for Marine Mineral Resources, Qingdao National Laboratory for Marine Science and Technology, Qingdao, China, [3]Swedish Museum of Natural History, Department of Palaeobiology, Stockholm, Sweden, [4]Ministry of Land and Resources of the People's Republic of China Key Laboratory of Marine Mineral Resources, Guangzhou Marine Geological Survey, Guangzhou, China

The natural dynamics of fluid flow at methane seeps and increasingly human activities influence the biogeochemistry of the microenvironment and further determine the activity of the chemosynthetic communities within these ecosystems. However, ways to reconstruct short-term fluid flow dynamics and to decipher the influence of scientific exploration at seeps are limited. In this study, we present high-resolution trace elements/Ca ratios (Li/Ca, Mg/Ca, Ti/Ca, Mn/Ca, Co/Ca, Cu/Ca, Zn/Ca, Sr/Ca, Zr/Ca, Mo/Ca, Ba/Ca, Th/Ca and U/Ca ratios) from the shells of two species of chemosymbiotic bivalves (the thiotrophic vesicomyid clam *Archivesica marissinica* and the methanotrophic mussel *Gigantidas haimaensis*) from the Haima cold seeps of the South China Sea. We found that the complex distribution patterns of some trace elements (Mg/Ca, Sr/Ca, Mo/Ca and U/Ca ratios) in *G. haimaensis* are largely controlled by mineral composition or age. The observation of Co/Ca and Ba/Ca ratios in both species indicate strong physiological and environmental control on the incorporation of trace elements during the biomineralization process. Besides, the distribution patterns of other trace elements provide information that can be used to discuss open issues such as the loss of trace elements after death of the bivalves, and the possible influence of human activities such as sediment disturbance. Overall, this study emphasizes the potential for using high-resolution element geochemistry of seep bivalve shells to reveal the physiological and environmental factors that control the growth of bivalves, and to elucidate the potential history of fluid discharge at cold seeps.

KEYWORDS

methane seep, bivalve, bioarchive, trace elements, South China Sea

Introduction

The cold seep system is dynamic in both time and space (Suess, 2020). At present, there is a basic understanding of the activity rhythm of cold seep system on a long-time scale (millennia and above, Chen et al., 2019). Yet, increasing evidence points to short-term events such as tides or monsoons also having an influence on methane flux (Himmler et al., 2016; Wang, S. et al., 2020), but the overall frequency of such microenvironmental changes in cold seep systems remains unclear (Leifer et al., 2004; Johansen et al., 2017).

The bivalve shell is an excellent archive to reveal the evolution of their living environment on a relatively short timescale because the lifespan of bivalves can range from several to hundreds of years (Barry et al., 2007; Schöne et al., 2013). As opposed to the soft tissue of bivalves, the corresponding shell is likely to integrate and preserve elements from their environment during their whole life (Immenhauser et al., 2015). Indeed, shell carbonate layers of bivalves can provide insights into various environmental conditions during their lifetime, while soft tissue can only give us instantaneous snapshots at a certain time (Vander Putten et al., 2000; Gillikin et al., 2006; Schöne et al., 2013; Feng et al., 2018; Wang, X. et al., 2020).

Numerous studies have shown that elemental compositions in shell carbonates can provide valuable insights into past environments. Previous studies have successfully established the relationship between Sr/Ca (or Mg/Ca) and temperature, although these relationships may vary greatly among or within species (Branson et al., 2018). An alternative temperature proxy (Sr/Li ratio) was developed (Juárez-Aguilar et al., 2019), and the vital effects of Sr and Li incorporation into aragonite shells can be reduced by normalizing Sr/Ca to Li/Ca. In addition, the shell Mn/Ca ratio (Marali et al., 2017), Ba/Ca ratio (Gillikin et al., 2006; Schöne et al., 2013) and U/Ca (Kim et al., 2015; Poitevin et al., 2020) ratio were also thoroughly investigated as potential indicators of diagenetic trends, weathering intensity, salinity, paleoproductivity, pH and so on. However, the calcifying fluid chemistry and the corresponding mechanistic of shell formation appear to involve complex physiological responses and geochemical controls (e.g., Vander Putten et al., 2000; Schöne et al., 2013; Marali et al., 2017; Markulin et al., 2020). To date, only a few studies explored the high-resolution element geochemistry of deep-sea bivalve shells (Schöne and Giere, 2005; Shirai et al., 2008; Wisshak et al., 2009), and only one of them focused on cold seep areas (Torres et al., 2001). Torres et al. (2001) investigated shells of the vesicomyid clam *Calyptogena kilmeri* from seep sites in Monterey canyon (California, USA) and confirmed that clamshells can be used as paleotracers of fluid seepage events. However, they only investigated the Ba/Ca ratio of this chemoautotrophic bivalve. Lietard and Pierre (2008) performed a high-resolution stable isotope ($\delta^{18}O$ and $\delta^{13}C$) and cathodoluminescence study of lucinid bivalve shells (*Myrtea* aff. *amorpha*) from methane seeps in the Eastern Mediterranean Sea and demonstrated the potential of these methods to reconstruct methane release event, although the influence of metabolic effect could not be completely ruled out.

In the present study, we investigated two species of chemosymbiotic bivalves from the South China Sea. Using microstructure and high-resolution element geochemistry of their shells, the purpose of this study was to reconstruct short-term fluid flow dynamics and to shed light on the short-term microenvironmental changes of cold seep ecosystems.

Materials and methods

Sample collection and preservation

Specimens of two species of seep-restricted, chemosymbiotic bivalves (*Archivesica marissinica*: thiotrophic, infaunal; and *Gigantidas haimaensis*: methanotrophic, epifaunal or semi-infaunal) were collected at the active Haima cold-seep area (water depth: ~1400 m) in the northwestern South China Sea (Figure 1; Liang et al., 2017). Once onboard the ship, the soft tissue and corresponding shell of bivalves were dissected and washed with deionized water to remove salt. The shells were air-dried and placed in a sealed sample bag for analysis.

Shell preparation

It impossible to create a shell chronology for the specimens since the absolute growth rate of seep bivalves is currently unknown. In an attempt to record a longer life history, 4 relatively large individuals with the length between 12.5 and 16.8 cm (*A. marissinica*: C2015 + C2020; *G. haimaensis*: M2020 + M2021) were chosen for this study. The relationships between length, width and height among the two species are almost the same, illustrating that they grew freely and were not limited by additional factors (Table 1). To obtain cross section of bivalves, we used a diamond saw to slice the shells along the axis of maximal growth, following the prevailing practice (Vander Putten et al., 2000; Torres et al., 2001; Markulin et al., 2020). To determine the shell microstructure and facilitate the laser ablation analysis, the cross section of the shells was polished with silicon carbide sandpaper (2000Cw, Ying Qiu Brand).

Analytical procedure

Scanning electron microscopy

A Coxem EM30 PLUS SEM system (South Korea) with an accelerating voltage of 15 kV was used to observe the microstructures of *A. marissinica* and *G. haimaensis* at Shanghai Ocean University. Shell fragments from several

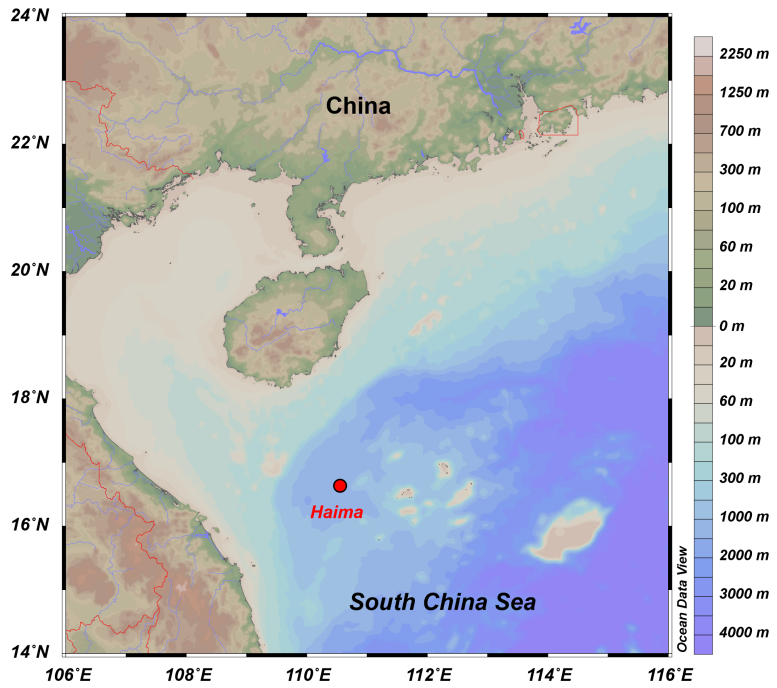

FIGURE 1
Map showing the location of the samples.

sections along the cross sections of each species were sputter-coated with a gold layer prior to observation, and the magnification varied from 969 to 2600 times (Figure 3).

X-ray diffraction

A LabX XRD-6100 X-ray diffractometer system (Shimadzu, Japan) at Shanghai Ocean University was used to analyze the mineral composition of bulk shells (individual microstructures could not be separated since the extremely thin thickness of shell). Approximately 40 mg shell powder was prepared for each sample. The X-ray source was a Cu anode operated at 40 kV and 30 mA using CuKα radiation equipped with a diffracted beam graphite monochromator. The samples were scanned in step scan mode at an interval of 10-80° (2θ), with a step size of 0.02° and a count time of 0.6 s per step (2°/min). The diverging, scattering, and receiving slits were 1.0 mm, 1.0 mm and 0.15 mm, respectively. The carbonate type of shells was identified by using XRD processing software JADE 6.0.

LA-ICP-MS

The concentrations of Li, Mg, Ca, Ti, Mn, Co, Cu, Zn, Sr, Zr, Mo, Ba, Th, and U were determined by means of laser ablation-inductively coupled plasma-mass spectrometry (LA-ICP-MS) in spot analysis mode along the growth axis of the shells near their outside layer (Figures 2C, D). The distance between the two laser spots is about 1mm (Figure 2), although the time span represented by two laser spots between shells or even in same shell, is different (bivalve grow faster when they were young). According to the sample size, the number of laser spots is 153 (C2015),111 (C2020),116 (M2020) and144 (M2021), respectively (Table 1). Analyses were performed at Shanghai Chemlabprop Technology Co., Ltd. using an ESI

TABLE 1 Seep bivalve information including: (1) species; (2) chemoautotrophic type; (3) length, (4) width, (5) height and (6) thickness of shells; (7) sampling time; (8) status when sampling; (9) total laser spots.

Sample ID	Species	Chemoautotrophic type	Length (cm)	Width (cm)	Height (cm)	Thickness (mm)	Sampling time	Status when sampling	Total laser spots
C2015	*Archivesica marissinica*	Thiotrophic clam	16.8	8.4	3.6	2.35	2015.04	Dead	153
C2020			13.5	6.7	2.9	1.92	2020.05	Alive	111
M2020	*Gigantidas platifrons*	Methanotrophic mussel	12.5	6.3	2.7	0.57	2020.05	Alive	116
M2021			16.1	8.1	3.5	0.71	2021.04	Alive	144

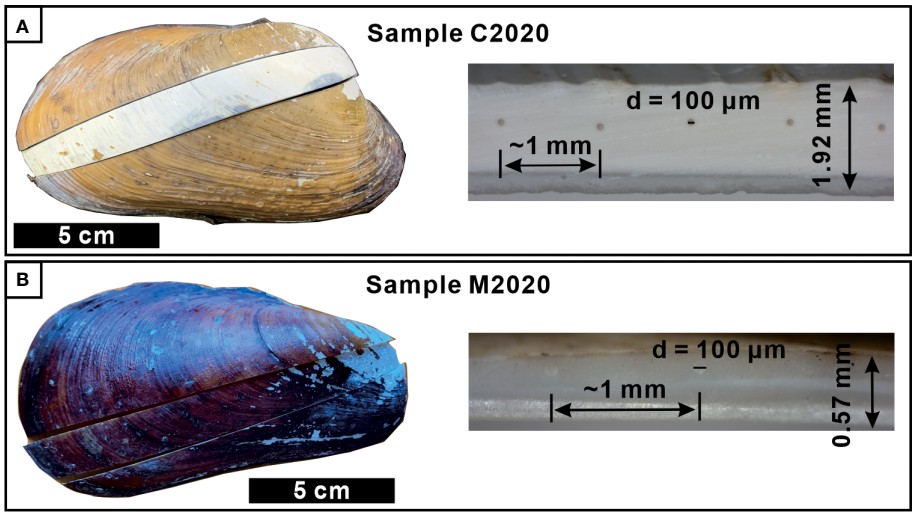

FIGURE 2
Images of typical seep bivalve shells and their cross sections. Clam identified as *Archivesica marissinica* (C2020; **A**) and mussel identified as *Gigantidas haimaensis* (M2020; **B**). The distance between two laser points is about 1 mm.

NWR193 ArF excimer laser ablation system equipped with a TwoVol2 ablation cell operating at 193 nm wavelength connected to an Agilent 7900 quadrupole ICP-MS. High-energy laser pulses hit the sample surface, and high-purity helium (99.999%) was used as the carrier gas at 700 ml/min flow to transfer the ablated material to the ICP for ionization before analysis. Satisfactory sensitivity and sufficiently low levels of oxide formation (ThO/Th < 0.2%) and fractionation effect ($^{232}Th/^{238}U \approx 100\%$) were accomplished by daily optimization, consisting of adjusting the gas flow, sampling depth, and lens setting while ablating the glass standard reference material NIST SRM 612. The ablation was operated using a spot size of 100 μm, an energy density of ~3 J/cm2 and a pulse repetition rate of 15 Hz. The background signal was measured for 10 s prior to each ablation. Ablation time was 50 s, followed by 15 s wash out. The operational conditions of LA-ICP-MS are summarized in Table S1.

To ensure the data quality, NIST SRM 612 glass reference material was used as the quality monitoring standard. The data were exported after being processed with the Iolite 4 software (Paton et al., 2011), and the measured values are shown in Table S2.

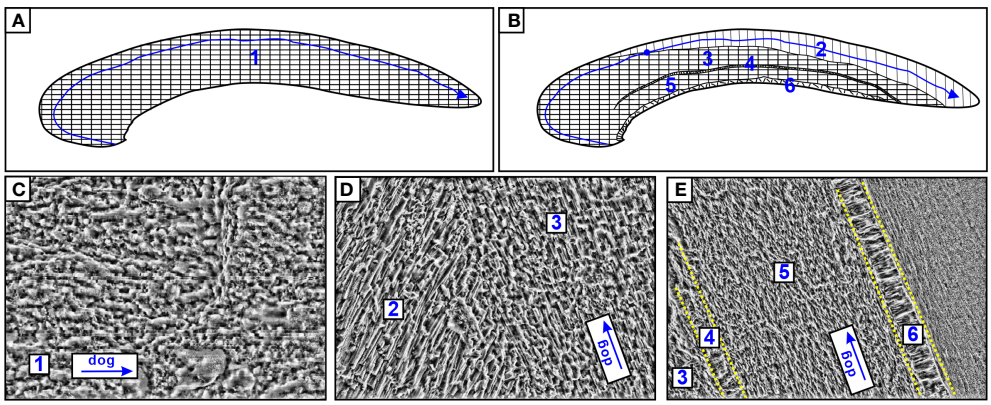

FIGURE 3
Schematic drawing of *A. marissinica* **(A)** and *G. haimaensis* **(B)**. The numbers represent laminated structures (1), outer prismatic layer (2), outer nacre layer (3), myostracum (4), inner nacre layer (5) and simple prismatic layer (6). The blue line with arrow represents the path of the laser spot, the blue point represents the transition position of mineral phase (aragonite to calcite). **(C)** SEM image of *A. marissinica* (C2020); **(D, E)** SEM image of *G. haimaensis* (M2020). dog: direction of growth.

Results

Shell microstructure of the seep bivalves

The thickness of the methanotrophic mussel shell (M2020: 0.57mm; M2021: 0.71mm) was less than one-third that of the thiotrophic clam shell (C2015: 2.35mm; C2020: 1.92mm. Table 1, Figures 2C, D). The microstructure of *A. marissinica* is rather simple since the whole shell is composed of a uniform laminated structure, the orientation of the laminae is consistent with the direction of growth (Figures 3A, C). The shell of *G. haimaensis* can be roughly divided into 5 parts from outside to inside layers (Figure 3): outer (fibrous) prismatic layer → outer nacre layer → myostracum → inner nacre layer → simple prismatic layer (Génio et al., 2012). Specifically, the fibers of the outer prismatic layer are oriented at an oblique angle to the outer nacreous layer. Between the outer and inner nacre layers, there is myostracum - a thin extra layer secreted by virtually all bivalves where they attach the mantle or the muscles to the shell. The inner edge of shell is a simple prismatic layer, a universal microstructure among mussels (family Mytilidae), with the prisms oriented vertically to the inner nacreous layer (Génio et al., 2012).

Carbonate mineral compositions

The mineral compositions of the two seep bivalves correspond to the properties of their microstructure. XRD results of *A. marissinica* show that the shell consists solely of aragonite, while the shell of *G. haimaensis* is composed of calcite and aragonite (Table S3). According to microstructure of the shell and previous research experience (Kennish et al., 1996; Kennish et al., 1998a; Kennish et al., 1998b), it is inferred that the fibrous prismatic layer of *G. haimaensis* is composed of calcite while the other layers are aragonitic (Génio et al., 2012; Immenhauser et al., 2015). The transition from aragonite phase to calcite phase of M2020 and M2021 occurred at laser point 40 and 46, respectively.

Element concentrations

Element results were reported in the form of trace element/calcium (TE/Ca) ratios in Table S4. The Mg/Ca ratio of *G. haimaensis* (~200-14000 μmol/mol, seawater at Sanya Bay: ~4900-5400 μmol/mol, Wu et al., 2014) is significantly higher than that of *A. marissinica* (~100-1200 μmol/mol, pore water at Haima active cold seep area: ~5300-17700 μmol/mol, Wang et al., 2018), which is quite different from the Mg/Ca ratio of their living environments. In addition, the ranges of other element concentrations of the two species were very similar (Figures 4–6).

Discussion

Factors controlling TE/Ca ratios of seep bivalve shells

The factors driving the incorporation of trace elements into bivalve shells are complex and mainly include environmental factors (e.g., temperature, salinity, organic matter, microstructure, nutrition, pollution, etc.) and physiological regulation (e.g., mineral composition, growth rate, etc., Vander Putten et al., 2000; Gillikin et al., 2006; Shirai et al., 2014). Bivalves from shallow and deep-sea are facing different survival pressures. Compared to the shallow bivalves, the living environment for deep sea bivalves is relatively stable and the survival challenge mainly comes from food supply (Wisshak et al., 2009). Although a continuous line of sampling points intuitively suggests a time series with an equal amount of time between each point, the time interval between two sample points in the late stage of growth was much longer than at the beginning of growth, because bivalves grow much faster in their early stage and considerably slower when they get older (Barry et al., 2007). In addition, the faster the growth rate of the bivalve, the less physiological control it has over how much trace elements are incorporated into the shell. Our discussion is based on the relative age framework of the shell and draws on the achievements of previous studies (Vander Putten et al., 2000; Gillikin et al., 2006).

The mineral composition of shell carbonate is controlled by physiological regulation. The Mg/Ca and Sr/Ca ratios show an inverse pattern in *G. haimaensis* and remain constant in *A. marissinica* (Figures 4A2, B2). This is consistent with the fact that most of the derived heterodont bivalves shell (to which the vesicomyids belong) is aragonite and mussel shell (Family mytilids) is the mixture of calcite and aragonite. In *G. haimaensis*, the outer, calcitic layer near the umbones is so thin that it could not be targeted by our sampling method. Thus at a specific position (blue dot in Figure 3B, point 40 for M2020 and point 46 for M2021), our LA-ICP-MS sampling points moved from the aragonitic nacre layer into the calcitic outer layer, resulting in obvious changes in the Mg/Ca and Sr/Ca ratios (Figures 4A2, B2). Aragonite is generally richer in Sr than calcite. However, interestingly, the Sr/Ca ratios of *A. marissinica* is similar to the calcitic part of *G. haimaensis* but much lower than its aragonitic part, highlights the strong physiological control on the incorporation of Sr into seep bivalve shells.

Molybdenum (Mo) enrichment in cold seep systems is a very common and useful trace element proxy (Wang et al., 2019). The behavior of Mo in pore water changes when the H_2S concentration exceeds 11 μM, and Mo in pore water will be scavenged and enter the sediment and then be captured by pyrite, resulting in a sharp decrease in Mo in pore water (Helz

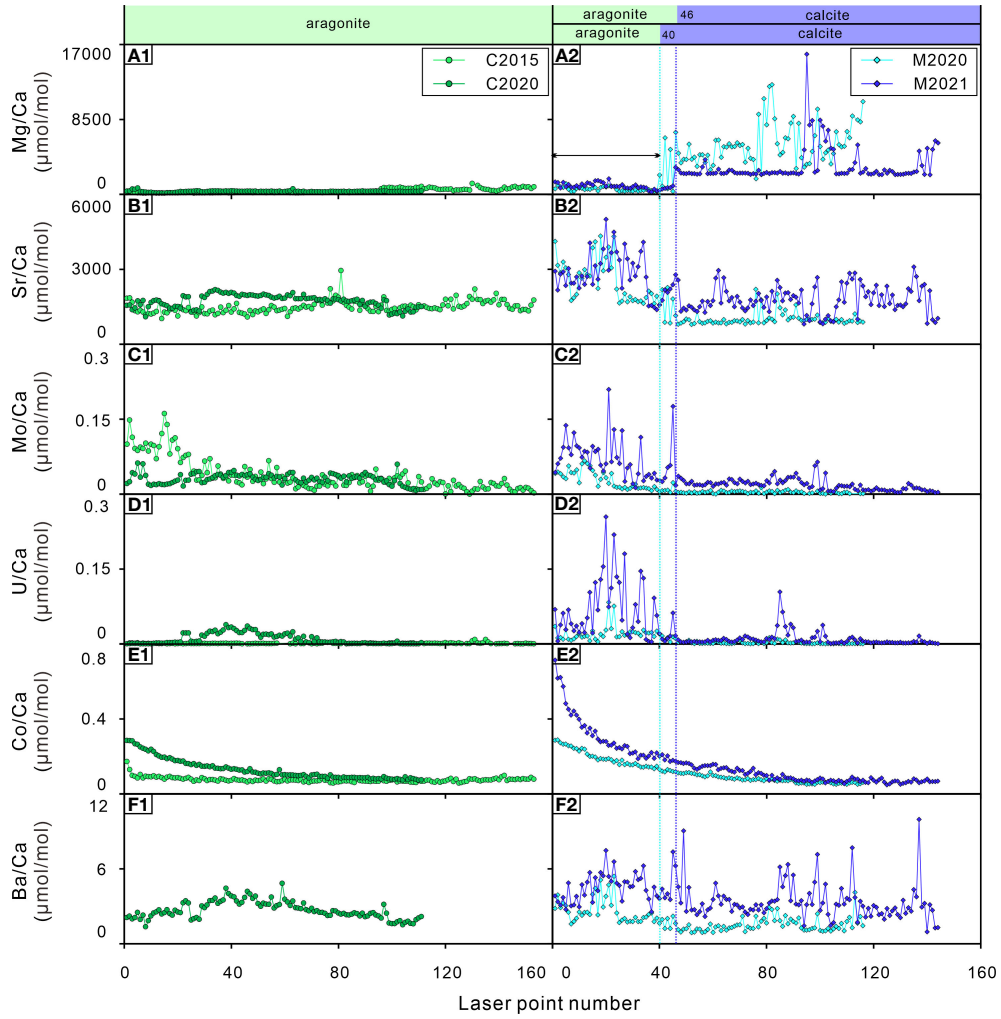

FIGURE 4
Elements/Ca ratios of the bivalve shells. **(A1, A2)** Mg/Ca ratios; **(B1, B2)** Sr/Ca ratios; **(C1, C2)** Mo/Ca ratios; **(D1, D2)** U/Ca ratios; **(E1, E2)** Co/Ca ratios; **(F1, F2)** Ba/Ca ratios. C2015 and C2020 are *A. marissinica*; M2020 and M2021 are *G. haimaensis*. The blue dotted lines indicate the change from aragonite to calcite in *G. haimaensis*.

et al., 1996). In this study, except for C2020, the Mo/Ca ratios of the bivalve shells were higher in their early stage of life and then gradually decreased with occasional peaks. Visually, the Mo/Ca ratio of *G. haimaensis* is probably related to their Mg/Ca and Sr/Ca ratios (i.e. mineral composition). However, the trend of Mo/Ca ratio is inconsistent with the theoretical calculation based on density functional theory (incorporation stability of molybdate anions: calcite > aragonite. Midgley et al., 2020), and there is also no difference of Mo concentration in aragonite versus calcite (Wang et al., 2019). For bivalves, it was found that the incorporation of Mo into the shell is influenced by the growth rate (Tabouret et al., 2012). Therefore, a simple explanation for the Mo pattern observed here is that the bivalves get more control over Mo incorporation with age. However, this is not the case for C2020; possibly, Mo concentration were lower during its early life. Interestingly, there is virtually no difference in Mo concentration between the infaunal (=living within the sediment) *A. marissinica* and the epifaunal *G. haimaensis* (Figures 4C1, C2).

The U/Ca ratios of seep bivalves seem to be closely related to their corresponding Sr/Ca ratios, implying that the incorporation of U into shells could be related to mineral composition (Figure 4, Cravo et al., 2002). It is also found that the U/Ca ratio of marine bivalve shells is higher in the early stage of life but drops below the detection limit in the later stage due to vital effects (Gillikin and Dehairs, 2013). Therefore, as far as the seep-inhabiting species investigated here are concerned, the U/Ca ratios could be regulated by physiological factors, especially among *G. haimaensis*.

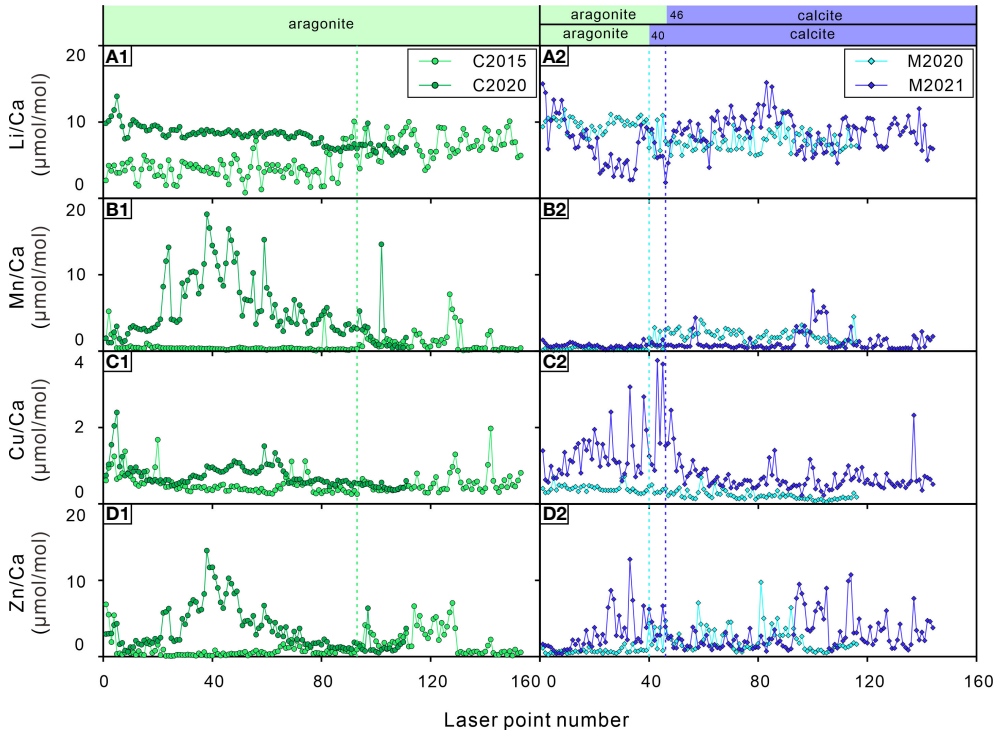

FIGURE 5
Elements/Ca ratios of the bivalve shells. **(A1, A2)** Li/Ca ratios; **(B1, B2)** Mn/Ca ratios; **(C1, C2)** Cu/Ca ratios; **(D1, D2)** Zn/Ca ratios. C2015 and C2020 are *A. marissinica* while M2020 and M2021 are *G. haimaensis*. The blue dotted lines indicate the change from aragonite to calcite in *G. haimaensis*, the green dotted line represents the boundary where elements may be lost for C2015.

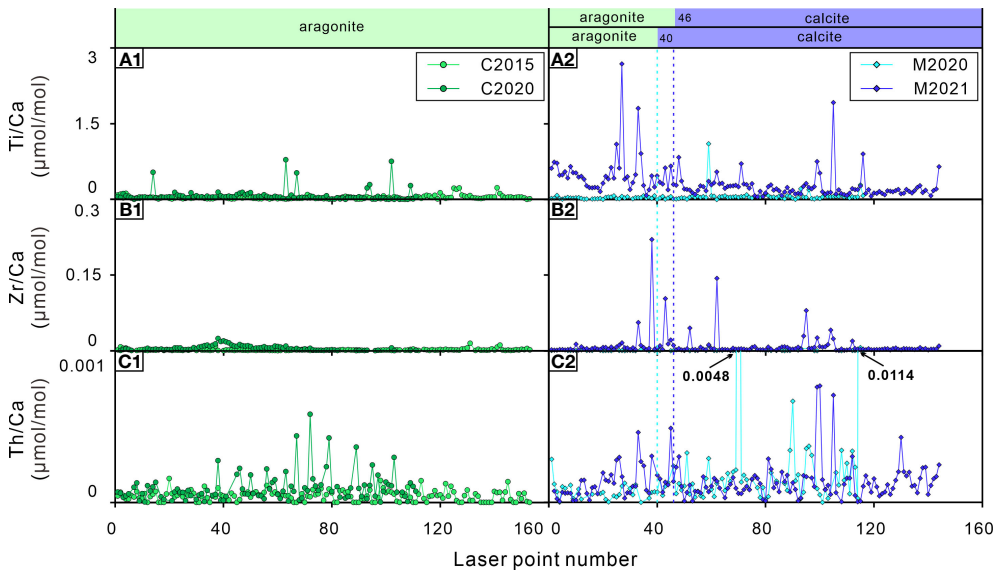

FIGURE 6
Elements/Ca ratios of the bivalve shells. **(A1, A2)** Ti/Ca ratios; **(B1, B2)** Zr/Ca ratios; **(C1, C2)** Th/Ca ratios. C2015 and C2020 are *A. marissinica* while M2020 and M2021 are *G. haimaensis*. The blue dotted lines indicate the change from aragonite to calcite in *G. haimaensis*.

Cobalt (Co) is a biologically essential element (Saito et al., 2004). Co^{2+} competes with Ca^{2+} ions during biomineralization (Bellotto and Miekeley, 2007; Honig et al., 2020). Co is a vital component of vitamin B12 (cyanocobalamin), which is a coenzyme in many cellular processes, including the synthesis of DNA and the oxidation of fatty acids (Blust, 2011; Pouil et al., 2017). There are few exhaustive studies of Co on the physiological effect of bivalves thus far. Previous research indicates that the changes in lipid and sterol metabolism increased with increasing Co^{2+} concentrations, and it is possible that Co^{2+} provokes oxidation damage in mussels (Nechev et al., 2006). Another study showed that the concentration of Co in the clam *Ruditapes philippinarum* increases with increasing CO2 (acidified seawater, Sezer et al., 2018). In a recent study, Honig et al. (2020) found that several TE/Ca ratios differed significantly between age classes, and Co/Ca ratios were usually greater in larvae than in juveniles. It can be determined that the incorporation of Co into shell carbonate is physiologically regulated. With increasing age, the Co/Ca ratios of the shells exponentially decline in both bivalves (Figures 4E1, E2). As far as we know, there is no unambiguous knowledge of this trend. The most likely scenario is that the cobalt-assimilation rate of bivalves slows down with age. Based on this observation, we suppose that the Co/Ca ratios of seep bivalve shells have the potential to be a tool to calculate the age of bivalves at seeps, as long as we obtain the age-confirmed sample and ascertain the function between the age and Co/Ca ratios of seep bivalves. However, the potential of this approach needs to be validated in other seep areas.

The Ba/Ca ratios of shallow-water bivalve shells have been used to reconstruct the primary productivity of their living environment, which is often related to phytoplankton blooms (Vander Putten et al., 2000; Kelemen et al., 2019; Fröhlich et al., 2022), the amplitude of the chlorophyll peaks is often used to explain the peak value of the Ba/Ca ratio of bivalve shells (Goodwin et al., 2013; Doré et al., 2020). Therefore, as long as the Ba/Ca ratio of bivalve shells is not strongly physiologically controlled, the change in Ba in the environment can be reflected in shells because the Ba/Ca ratio of bivalve shells is usually related to the Ba/Ca ratio of environmental water (Gillikin et al., 2006; Goodwin et al., 2013). There are many factors that lead to an increase in Ba in the environment. In addition to autochthonic effects, such as the formation of barite ($BaSO_4$) crystals caused by flocs after phytoplankton decay (Doré et al., 2020), autochthonic effects also include the addition of Ba-rich external fluids to the environment (such as freshwater, groundwater, hydrothermal fluids, upwelling caused by typhoons and storms, etc. Shirai et al., 2008; Goodwin et al., 2013; Markulin et al., 2020), which may lead to changes in salinity in the environment. As mentioned by some previous studies, Ba/Ca ratios in bivalve shells can be used to track salinity (Gillikin et al., 2006; Poulain et al., 2015). The Ba/Ca ratios of C2020 (*A. marissinica*) have a relatively flat distribution pattern with lower values (Ba/Ca ratios of C2015 is below detection limit) while the Ba/Ca ratios of *G. haimaensis* exhibit notable fluctuations with uncertain cycles and large relative amplitudes. The Ba/Ca ratio pattern of *G. haimaensis* appears to be typical for bivalves, as it has been recognized in almost all Ba/Ca ratio profiles of bivalve shells — relatively stable for most of their lifetime interrupted by occasional sharp peaks (Gillikin et al., 2008; Schöne et al., 2013; Poulain et al., 2015; Marali et al., 2017; Markulin et al., 2020). The study site is an area of active seepage with an obvious Ba front in the sediment (the highest concentration of Ba is ~1200 ppm, Liu, S et al., 2020), indicating a considerable Ba supply. Therefore, in our opinion, the peak Ba/Ca ratios of seep bivalves are affected by the discharge of Ba-rich fluids. The same conclusion was reached by Torres et al. (2001), although the peak Ba/Ca ratio in our study (10 μmol/mol) is much lower than theirs (up to 80 μmol/mol). It is necessary to analyze more shells collected from the same cold seep area in the future. If there is strong interindividual reproducibility of the Ba/Ca ratio, then environmental driving factors that control the incorporation of Ba in shells exist.

In summary, due to its monomineralic composition, the distribution of trace elements in *A. marissinica* has its unique advantages in constraining physiological mechanism and reconstructing the changes of microenvironment in the study area. The distribution of trace elements in the bimineralic *G. haimaensis* and other mussel shells is easily affected by mineral composition, as reflected in the Mg/Ca and Sr/Ca ratios, and potentially the U/Ca ratios, too. To solve the issues with bimineralic shells encountered in this study, the application of chemical staining could be used to distinguish aragonite from calcite in future research (Kato et al., 2003). In addition, we propose that the Mo/Ca ratios in the studies bivalves were controlled by age (i.e. growth rate), and probably affected by environmental factors (for C2020). The Co/Ca ratios of seep bivalve shells intuitively indicates that the rate of Co incorporated into the shell carbonate slows down with age, opening the potential to utilize this trend to constrain the age of seep bivalves.

Loss of trace elements in shells after death of the bivalves?

Based on the observation of some TE/Ca ratios of C2015, there is the potential of element loss (decline in concentration) after the bivalve dies. At the time of collection, C2015 was the only dead individual of all four samples. Compared to the other three bivalve shells, the TE/Ca ratios of C2015 often show a flatter distribution pattern (Figure 5). As mentioned earlier, the Mg/Ca and Sr/Ca ratios of seep bivalve shells are mainly

controlled by physiological factors. The mineral composition of C2015 is aragonite, and the ratios of Mg/Ca and Sr/Ca should be relatively stable if there are no other factors involved. This is true for the Sr/Ca ratio but not for the Mg/Ca ratio. After laser point 93, the Mg/Ca ratio of C2015 was significantly increased, implying that Mg may lost before laser point 93 (Figure 4). The same patterns are also observed for the Li/Ca, Mn/Ca, Cu/Ca and Zn/Ca ratios, which all exhibit lower ratios before laser point 93 (green dot line in Figure 5). Furthermore, the decreasing trend of the Co/Ca ratio of C2015 stopped at point 3 (Figure 4E1), which is obviously different from the logarithmic decreasing trend of the other three samples. The Ba/Ca ratios of C2015 were not reported because the content of Ba is lower than the detection limit. Therefore, Co and Ba may also be lost. A possibility is that these trace elements are actually contained in the organic matter within the shell. The presence of organic matter occupies the position of lattice in bivalve shells, thus affect the contents of lattice-bound trace elements. At the same time, trace elements can be adsorbed on organic matter of the shell (Roditi et al., 2000; Vander Putten et al., 2000). It has been observed that organic matter degradation effects the contents of Mn, Mg, Sr and Pb in shells (Takesue et al., 2008). The collected fresh shells obviously contained more organic matter, whereas in C2015, the organic matter had already decayed. It is of course also possible that this phenomenon is caused by individual differences (for example, the M2021 overall has a flatter distribution of Mn/Ca than M2020, whereas M2020 has a much flatter distribution of Cu/Ca compared to M2021), follow-up research is needed on this issue.

The potential influence of human activity on cold seep systems

With the further expansion of human activities to deep-sea cold seep areas, such as fishing, onshore and offshore mining, pollution, and also scientific investigation, these ecosystems are increasingly threatened. For example, epifaunal seep communities on the Hikurangi Margin were disturbed by bottom trawling (Bowden et al., 2013), seep faunas off of northern Papua New Guinea are affected by tailings from onshore mining (Samadi et al., 2015), mining of gas hydrates is explored along continental margins (Song et al., 2014), and trash and other leftovers of human activities are found at increasingly great depth (Schlining et al., 2013). Unfortunately, the deep sea is a slow world, which is not only manifested in the slow growth of various microorganisms, but also in the slow recovery of the environment after being changed (Neves et al., 2015). Now, this tendency has drawn the attention of some countries and international organizations (Van Dover et al., 2012; Danovaro et al., 2020). For example, the Croker Carbonate Slabs in the Irish Sea, as "submarine structures formed by leaking gases", have been designated as a marine protected area (MPA) under the European Commission's Habitats Directive (Judd et al., 2020).

At an active cold seep site in the South China Sea, called 'site F', Wang et al. (2017) found that the concentrations of K, Mg, Sr, Cu, Mo and V increased toward the outer edge of bivalve shells, indicating more abundant concentrations of trace metals in ambient seawater in recent years, which suggests that human activities may interfere with the cold seep area. The studies of tubeworms in cold seep area also found that the top and root of the tubeworms were strongly affected by the environment, causing the anomaly of some redox sensitive elements and rare earth elements (Duperron et al., 2014; Bayon et al., 2020).

A noteworthy phenomenon in this study is that there are abnormal Ti/Ca, Zr/Ca and Th/Ca ratio peaks in bivalve shells C2020, M2020 and M2021, but there are virtually no such peaks in C2015 (Figure 6). As far as we know, there is no report of the biological utilization of elements such as Ti, Zr and Th. Since these are typical elements of terrigenous sediments, one could propose that a drastic increase of these ratios in the bivalve shells was induced by their variability of the bivalves' living environment. Since the discovery of "Haima" cold seeps in 2015, scientific research activities at this site have become an annual event. It is common for ROV cruise to Haima cold seep, and the frequency is increasing year by year (Liang et al., 2017; Wang et al., 2022). When the submersible is maneuvering or sampling, it induces large 'dust clouds', which will slowly settle on the seabed (Figure 7). We suspect that these activities affected the submarine cold seep ecosystem and have been written down into the trace element record of the bivalve shells to a certain extent.

Conclusion and implication

Analysis of high-resolution element geochemistry of shells of two species of seep bivalve from the Haima cold seeps in the South China Sea confirms that these shells are biogeochemical recorder of short-term environmental change and physiological parameters at cold seeps. The incorporation of trace elements such as Mg, Sr, Mo, U, Co, Ba in seep bivalve shells is mainly controlled by physiological and environmental factors; the distribution of Co could potentially be developed into an independent index to estimate the age of seep bivalves. Notwithstanding limitations, our results put forward some open questions concerning the element loss for dead shell (Li-Mn-Cu-Zn) and the influence of human activity on cold seep systems (Ti-Zr-Th). We propose the necessity to investigate seep bivalves on the basis of an absolute age framework and to understand their physiological characteristics in the future, which is a

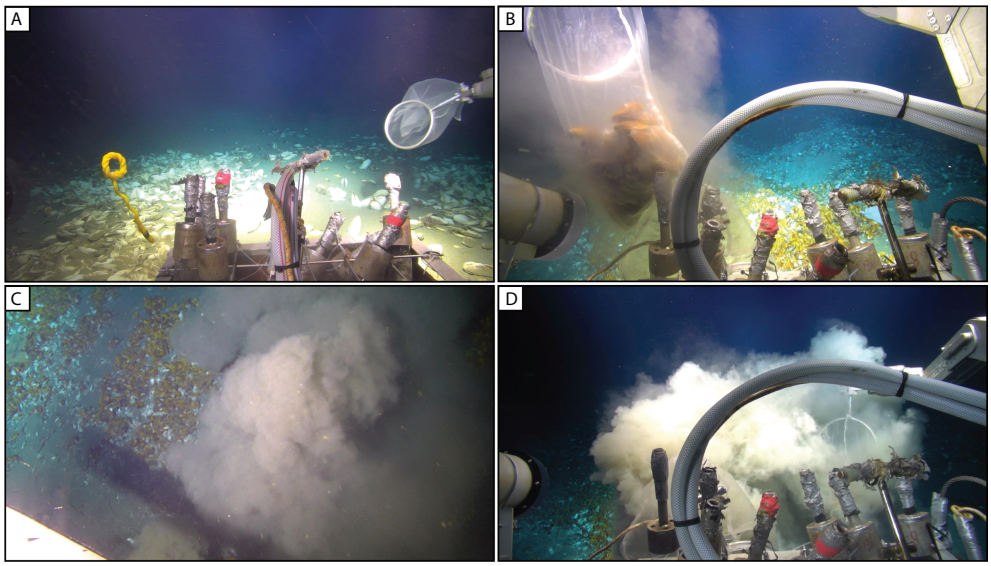

FIGURE 7
Seafloor images showing the 'dust clouds' caused by the ROV during sampling. **(A)** Field of live and dead vesicomyid clams; **(B–D)** large bathymodiolin mussel beds.

prerequisite for further determining the unique potential and effectiveness of this bioarchive in reconstructing environmental information on cold seep systems in a short time scale (years to decades). This study has examined only limited samples that span a relatively short time, our conclusions may thus reflect localized conditions only. Through more measurements over a larger area and longer timespan, the interactions between seep animals and the local environments may be further verified.

Data availability statement

The datasets presented in this study can be found in online repositories. The names of the repository/repositories and accession number(s) can be found in the article/ Supplementary Material.

Author contributions

XW: conceptualization, methodology, data analysis, and writing-original manuscript. DaF: methodology. SK: writing-review & editing. SG: sample collection. QL: sample collection. JT: sample collection. DC: data analysis. DoF: conceptualization, supervision, funding acquisition, and writing-review & editing. All authors contributed to manuscript preparation. All authors contributed to the article and approved the submitted version.

Funding

This study was partially sponsored by the National Natural Science Foundation of China (Grants: 41730528, 42106059, 42225603), Shanghai Sailing Program (Grant: 21YF1416800), special funding for the development of science and technology of Shanghai Ocean University and startup foundation for young teachers of Shanghai Ocean University.

Acknowledgments

The crew and captain of the *Haiyang-6* research vessel and *Haima* ROV are thanked for sample collection. We are grateful to Zice Jia (SHOU) for XRD measurement.

Conflict of interest

The authors declare that the research was conducted in the absence of any commercial or financial relationships that could be construed as a potential conflict of interest.

Publisher's note

All claims expressed in this article are solely those of the authors and do not necessarily represent those of their

affiliated organizations, or those of the publisher, the editors and the reviewers. Any product that may be evaluated in this article, or claim that may be made by its manufacturer, is not guaranteed or endorsed by the publisher.

Supplementary material

The Supplementary Material for this article can be found online at: https://www.frontiersin.org/articles/10.3389/fmars.2022.960338/full#supplementary-material

References

Barry, J. P., Whaling, P. J., and Kochevar, R. K. (2007). Growth, production, and mortality of the chemosynthetic vesicomyid bivalve, calyptogena kilmeri from cold seeps off central California. *Mar. Ecol.* 28, 169–182. doi: 10.1111/j.1439-0485.2007.00119.x

Bayon, G., Lemaitre, N., Barrat, J.-A., Wang, X., Feng, D., and Duperron, S. (2020). Microbial utilization of rare earth elements at cold seeps related to aerobic methane oxidation. *Chem. Geol.* 555, 119832. doi: 10.1016/j.chemgeo.2020.119832

Bellotto, V., and Miekeley, N. (2007). Trace metals in mussel shells and corresponding soft tissue samples: a validation experiment for the use of perna perna shells in pollution monitoring. *Anal. Bioanal. Chem.* 389, 769–776. doi: 10.1007/s00216-007-1420-y

Blust, R. (2011). "Cobalt," in *Fish physiology: Homeostasis and toxicology of essential metals, 1st ed*. Eds. C. M. Wood, A. P. Farrell and C. J. Brauner (Amsterdam: Elsevier), 291–326.

Bowden, D. A., Rowden, A. A., Thurber, A. R., Baco, A. R., Levin, L. A., and Smith, C. R. (2013). Cold seep epifaunal communities on the hikurangi margin, new zealand: composition, succession, and vulnerability to human activities. *PloS One* 8, e76869. doi: 10.1371/journal.pone.0076869

Branson, O., Redfern, S. A. T., Elmore, A. C., Read, E., Valencia, S., and Elderfield, H. (2018). The distribution and coordination of trace elements in krithe ostracods and their implications for paleothermometry. *Geochim. Cosmochim. Acta* 236, 230–239. doi: 10.1016/j.gca.2017.12.005

Chen, F., Wang, X., Li, N., Cao, J., Bayon, G., Peckmann, J., et al. (2019). Gas hydrate dissociation during sea-level highstand inferred from U/Th dating of seep carbonate from the south China Sea. *Geophys. Res. Lett.* 46, 13928–13938. doi: 10.1029/2019GL085643

Cravo, A., Foster, P., and Bebianno, M. J. (2002). Minor and trace elements in the shell of patella aspera (Röding 1798). *Environ. Int.* 28, 295–302. doi: 10.1016/s0160-4120(02)00038-7

Danovaro, R., Fanelli, E., Aguzzi, J., Billett, D., Carugati, L., Corinaldesi, C., et al. (2020). Ecological variables for developing a global deep-ocean monitoring and conservation strategy. *Nat. Ecol. Evol.* 4, 181–192. doi: 10.1038/s41559-019-1091-z

Doré, J., Chaillou, G., Poitevin, P., Lazure, P., Poirier, A., Chauvaud, L., et al. (2020). Assessment of ba/ca in arctica islandica shells as a proxy for phytoplankton dynamics in the northwestern atlantic ocean. *Estuar. Coast. Shelf Sci.* 237, 106628. doi: 10.1016/j.ecss.2020.106628

Duperron, S., Gaudron, S. M., Lemaitre, N., and Bayon, G. (2014). A microbiological and biogeochemical investigation of the cold seep tubeworm escarpia southwardae (Annelida: Siboglinidae): symbiosis and trace element composition of the tube. *Deep-Sea Res. Part I-Oceanogr. Res. Pap.* 90, 105–114. doi: 10.1016/j.dsr.2014.05.006

Feng, D., Peckmann, P., Li, N., Kiel, S., Qiu, J.-W., Liang, Q., et al. (2018). The stable isotope fingerprint of chemosymbiosis in the shell organic matrix of seep-dwelling bivalves. *Chem. Geol.* 479, 241–250. doi: 10.1016/j.chemgeo.2018.01.015

Fröhlich, L., Siebert, V., Walliser, E. O., Thébault, J., Jochum, K. P., Chauvaud, L., et al. (2022). Ba/Ca profiles in shells of pecten maximus – a proxy for specific primary producers rather than bulk phytoplankton. *Chem. Geol* 593, 120743. doi: 10.1016/j.chemgeo.2022.120743

Génio, L., Kiel, S., Cunha, M. R., Grahame, J., and Little, C. T. S. (2012). Shell microstructures of mussels (Bivalvia: Mytilidae: Bathymodiolinae) from deep-sea chemosynthetic sites: Do they have a phylogenetic significance? *Deep-Sea Res. Part I-Oceanogr. Res. Pap.* 64, 86–103. doi: 10.1016/j.dsr.2012.02.002

Gillikin, D., and Dehairs, F. (2013). Uranium in aragonitic marine bivalve shells. *Palaeogeogr. Palaeoclimatol. Palaeoecol.* 373, 60–65. doi: 10.1016/j.palaeo.2012.02.028

Gillikin, D. P., Dehairs, F., Lorrain, A., Steenmans, D., Baeyens, W., and André, L. (2006). Barium uptake into the shells of the common mussel (Mytilus edulis) and the potential for estuarine paleo-chemistry reconstruction. *Geochim. Cosmochim. Acta* 70, 395–407. doi: 10.1016/j.gca.2005.09.015

Gillikin, D. P., Lorrain, A., Paulet, Y.-M., André, L., and Dehairs, F. (2008). Synchronous barium peaks in high-resolution profiles of calcite and aragonite marine bivalve shells. *Geo-Mar. Lett.* 28, 351–358. doi: 10.1007/s00367-008-0111-9

Goodwin, D. H., Gillikin, D. P., and Roopnarine, P. D. (2013). Preliminary evaluation of potential stable isotope and trace element productivity proxies in the oyster crassostrea gigas. *Palaeogeogr. Palaeoclimatol. Palaeoecol.* 373, 88–97. doi: 10.1016/j.palaeo.2012.03.034

Helz, G. R., Miller, C. V., Charnock, J. M., Mosselmans, J. F. W., Pattrick, R. A. D., Garner, C. D., et al. (1996). Mechanism of molybdenum removal from the sea and its concentration in black shales: EXAFS evidence. *Geochim. Cosmochim. Acta* 60, 3631–3642. doi: 10.1016/0016-7037(96)00195-0

Himmler, T., Bayon, G., Wangner, D., Enzmann, F., Peckmann, J., and Bohrmann, G. (2016). Seep-carbonate lamination controlled by cyclic particle flux. *Sci. Rep.* 6, 37439. doi: 10.1038/srep37439

Honig, A., Etter, R., Pepperman, K., Morello, S., and Hannigan, R. (2020). Site and age discrimination using trace element fingerprints in the blue mussel. *J. Exp. Mar. Biol. Ecol.* 522, 151249. doi: 10.1016/j.jembe.2019.151249

Immenhauser, A., Schöne, B. R., Hoffmann, R., and Niedermayr, A. (2015). Mollusc and brachiopod skeletal hard parts: Intricate archives of their marine environment. *Sedimentology* 63, 1–59. doi: 10.1111/sed.12231

Johansen, C., Todd, A. C., and MacDonald, I. R. (2017). Time series video analysis of bubble release processes at natural hydrocarbon seeps in the northern gulf of Mexico. *Mar. Pet. Geol.* 82, 21–34. doi: 10.1016/j.marpetgeo.2017.01.014

Juárez-Aguilar, E. A., Sánchez-Beristain, F., and Bernal, J. P. (2019). Determination of the temperature of precipitation of aragonite in shells of anadara brasiliana (Lamarck, 1819) from playa norte, cazones de herrera (Holocene, veracruz, Mexico) by means of trace element analysis. *J. South Am. Earth Sci.* 91, 71–79. doi: 10.1016/j.jsames.2019.01.007

Judd, A., Noble-James, T., Golding, N., Eggett, A., Diesing, M., Clare, D., et al. (2020). The croker carbonate slabs: extensive methane-derived authigenic carbonate in the Irish Sea–nature, origin, longevity and environmental significance. *Geo-Mar. Lett.* 40, 423–438. doi: 10.1007/s00367-019-00584-0

Kato, K., Wada, H., and Fujioka, K. (2003). The application of chemical staining to separate calcite and aragonite minerals for micro-scale isotopic analyses. *Geochem. J.* 37, 291–297. doi: 10.2343/geochemj.37.291

Kelemen, Z., Gillikin, D. P., and Bouillon, S. (2019). Relationship between river water chemistry and shell chemistry of two tropical African freshwater bivalve species. *Chem. Geol.* 526, 130–141. doi: 10.1016/j.chemgeo.2018.04.026

Kennish, M. J., Lutz, R. A., and Tan, A. S. (1998a). Deep-sea vesicomyid clams from hydrothermal vent and cold seep environments: analysis of shell microstructure. *Veliger* 41, 195–200.

Kennish, M. J., Tan, A. S., and Lutz, R. A. (1996). Shell microstructure of vesicomyid clams from various hydrothermal vent and cold seep environments. *Malacologia* 37, 363–373.

Kennish, M. J., Tan, A. S., and Lutz, R. A. (1998b). Shell microstructure of mytilids (Bivalvia) from deep-sea hydrothermal vents and cold-water sulfide/methane seep environments. *Nautilus* 112, 84–89.

Kim, B., Cheong, D., and Lee, E. (2015).). paleoenvironmental changes in northern Mongolia during the last deglaciation revealed by trace element records in ostracods from lake hovsgol. *Quat. Int.* 384, 169–179. doi: 10.1016/j.quaint.2015.04.041

Leifer, I., Boles, J. R., Luyendyk, B. P., and Clark, J. F. (2004). Transient discharges from marine hydrocarbon seeps: spatial and temporal variability. *Environ. Geol.* 46, 1038–1052. doi: 10.1007/s00254-004-1091-3

Liang, Q., Hu, Y., Feng, D., Peckmann, J., Chen, L., Yang, S., et al. (2017). Authigenic carbonates from newly discovered active cold seeps on the northwestern slope of the south China Sea: Constraints on fluid sources, formation environments, and seepage dynamics. *Deep-Sea Res. Part I-Oceanogr. Res. Pap.* 124, 31–41. doi: 10.1016/j.dsr.2017.04.015

Lietard, C., and Pierre, C. (2008). High-resolution isotopic records (δ18O and δ13C) and cathodoluminescence study of lucinid shells from methane seeps of the Eastern Mediterranean. *Geo-Mar Lett.* 28, 195–203. doi: 10.1007/s00367-008-0100-z

Liu, S., Feng, X., Feng, Z., Xiao, X., and Feng, L. (2020). Geochemical evidence of methane seepage in the sediments of the qiongdongnan basin, south China Sea. *Chem. Geol.* 543, 119588. doi: 10.1016/j.chemgeo.2020.119588

Marali, S., Schöne, B. R., Mertz-Kraus, R., Griffin, S. M., Wanamaker, A. D.Jr., Butler, P. G., et al. (2017). Reproducibility of trace element time-series (Na/Ca,Mg/Ca, Mn/Ca, Sr/Ca, and Ba/Ca) within and between specimens of the bivalve arctica islandica–a LA-ICP-MS line scan study. *Palaeogeogr. Palaeoclimatol. Palaeoecol.* 484, 109–128. doi: 10.1016/j.palaeo.2016.11.024

Markulin, K., Uvanović, H., Mertz-Kraus, R., Schöne, B. R., Kovač, Ž., Arapov, J., et al. (2020). Spatial variations in ba/cashell fingerprints of glycymeris pilosa along the eastern adriatic sea. *Estuar. Coast. Shelf Sci.* 243, 106821. doi: 10.1016/j.ecss.2020.106821

Midgley, S. D., Taylor, J. O., Fleitmann, D., and Grau-Crespo, R. (2020). Molybdenum and sulfur incorporation as oxyanion substitutional impurities in calcium carbonate minerals: A computational investigation. *Chem. Geol.* 553, 119796. doi: 10.1016/j.chemgeo.2020.119796

Nechev, J., Stefanov, K., and Popov, S. (2006). Effect of cobalt ions on lipid and sterol metabolism in the marine invertebrates mytilus galloprovincialis and actinia equina. *Comp. Biochem. Physiol. A-Mol. Integr. Physiol.* 144, 112–118. doi: 10.1016/j.cbpa.2006.02.022

Neves, B. M., Edinger, E., Layne, G. D., and Wareham, V. E. (2015). Decadal longevity and slow growth rates in the deep-water sea pen halipteris finmarchica (Sars, 1851) (Octocorallia: Pennatulacea): implications for vulnerability and recovery from anthropogenic disturbance. *Hydrobiologia* 759, 147–170. doi: 10.1007/s10750-015-2229-x

Paton, C., Hellstrom, J., Paul, B., Woodhead, J., and Hergt, J. (2011). Iolite: Freeware for the visualization and processing of mass spectrometer data. *J. Anal. At. Spectrom.* 26, 2508–2518. doi: 10.1039/C1JA10172B

Poitevin, P., Chauvaud, L., Pécheyran, C., Lazure, P., Jolivet, A., and Thébault, J. (2020). Does trace element composition of bivalve shells record utra-high frequency environmental variations? *Mar. Environ. Res.* 158, 104943. doi: 10.1016/j.marenvres.2020.104943

Pouil, S., Teyssié, J.-L., Rouleau, C., Fowler, S. W., Metian, M., Bustamante, P., et al. (2017). Comparative study of trophic transfer of the essential metals Co and zn in two tropical fish: A radiotracer approach. *J. Exp. Mar. Biol. Ecol.* 486, 42–51. doi: 10.1016/j.jembe.2016.09.005

Poulain, C., Gillikin, D. P., Thébault, J., Munaron, J. M., Bohn, M., Robert, R., et al. (2015). An evaluation of Mg/Ca, Sr/Ca, and Ba/Ca ratios as environmental proxies in aragonite bivalve shells. *Chem. Geol.* 396, 42–50. doi: 10.1016/j.chemgeo.2014.12.019

Roditi, H. A., Fisher, N. S., and Sañudo-Wilhelmy, S. A. (2000). Uptake of dissolved organic carbon and trace elements by zebra mussels. *Nature* 407, 78–80. doi: 10.1038/35024069

Saito, M. A., Moffett, J. W., and DiTullio, G. R. (2004). Cobalt and nickel in the Peru upwelling region: A major flux of labile cobalt utilized as a micronutrient. *Glob. Biogeochem. Cycle* 18, GB4030. doi: 10.1029/2003GB002216

Samadi, S., Puillandre, N., Pante, E., Boisselier, M.-C., Chen, W.-J., Corbari, L., et al. (2015). Patchiness of deep-sea communities in Papua new Guinea and potential susceptibility to anthropogenic disturbances illustrated by seep organisms. *Mar. Ecol.* 36, 109–132. doi: 10.1111/maec.12204

Schlining, K., von Thun, S., Kuhnz, L., Schlining, B., Lundsten, L., Stout, N. J., et al. (2013). Debris in the deep: Using a 22-year video annotation database to survey marine litter in monterey canyon, central california, usa. *Deep-Sea Res. Part I-Oceanogr. Res. Pap.* 79, 96–105. doi: 10.1016/j.dsr.2013.05.006

Schöne, B. R., and Giere, O. (2005). Growth increments and stable isotope variation in shells of the deep-sea hydrothermal vent bivalve mollusk bathymodiolus brevior from the north Fiji basin, pacific ocean. *Deep-Sea Res. Part I-Oceanogr. Res. Pap.* 52, 1896–1910. doi: 10.1016/j.dsr.2005.06.003

Schöne, B. R., Radermacher, P., Zhang, Z., and Jacob, D. E. (2013). Crystal fabrics and element impurities (Sr/Ca, Mg/Ca, and Ba/Ca) in shells of arctica islandica–implications for paleoclimate reconstructions. *Palaeogeogr. Palaeoclimatol. Palaeoecol.* 373, 50–59. doi: 10.1016/j.palaeo.2011.05.013

Sezer, N., Kocaoğlan, H. O., Lacoue-Labarthe, T., and Belivermiş, M. (2018). Acidified seawater increases accumulation of cobalt but not cesium in manila clam ruditapes philippinarum. *J. Environ. Radioact.* 184–185, 114–121. doi: 10.1016/j.jenvrad.2018.01.018

Shirai, K., Schöne, B. R., Miyaji, T., Radarmacher, P., Krause, R. A.Jr., and Tanabe, K. (2014). Assessment of the mechanism of elemental incorporation into bivalve shells (Arctica islandica) based on elemental distribution at the microstructural scale. *Geochim. Cosmochim. Acta* 126, 307–320. doi: 10.1016/j.gca.2013.10.050

Shirai, K., Takahata, N., Yamamoto, H., Omata, T., Sasaki, T., and Sano, Y. (2008). Novel analytical approach to bivalve shell biogeochemistry: A case study of hydrothermal mussel shell. *Geochem. J.* 42, 413–420. doi: 10.2343/GEOCHEMJ.42.413

Song, Y., Yang, L., Zhao, J., Liu, W., Yang, M., Li, Y., et al. (2014). The status of natural gas hydrate research in China: A review. *Renew. Sust. Energ. Rev.* 31, 778–791. doi: 10.1016/j.rser.2013.12.025

Suess, E. (2020). "Marine cold seeps: Background and recent advances," in *Hydrocarbons, oils and lipids: Diversity, origin, chemistry and fate*. Ed. H. Wilkes (Switzerland, Springer International Publishing, Cham), 747–767. doi: 10.1007/978-3-319-90569-3_27

Tabouret, H., Pomerleau, S., Jolivet, A., Pécheyran, C., Riso, R., Thébault, J., et al. (2012). Specific pathways for the incorporation of dissolved barium and molybdenum into the bivalve shell: An isotopic tracer approach in the juvenile great scallop (Pecten maximus). *Mar. Environ. Res.* 78, 15–25. doi: 10.1016/j.marenvres.2012.03.006

Takesue, R. K., Bacon, C. R., and Thompson, J. K. (2008). Influences of organic matter and calcification rate on trace elements in aragonitic estuarine bivalve shells. *Geochim. Cosmochim. Acta* 72, 5431–5445. doi: 10.1016/j.gca.2008.09.003

Torres, M. E., Barry, J. P., Hubbard, D. A., and Suess, E. (2001). Reconstructing the history of fluid flow at cold seep sites from Ba/Ca ratios in vesicomyid clam shells. *Limnol. Oceanogr.* 46, 1701–1708. doi: 10.4319/lo.2001.46.7.1701

Vander Putten, E., Dehairs, F., Keppens, E., and Baeyens, W. (2000). High resolution distribution of trace elements in the calcite shell layer of modern mytilus edulis: Environmental and biological controls. *Geochim. Cosmochim. Acta* 64, 997–1011. doi: 10.1016/S0016-7037(99)00380-4

Van Dover, C. L., Smith, C. R., Ardron, J., Dunn, D., Gjerde, K., Levin, L., et al. (2012). Designating networks of chemosynthetic ecosystem reserves in the deep sea. *Mar. Pol.* 36, 378–381. doi: 10.1016/j.marpol.2011.07.002

Wang, X., Barrat, J.-A., Bayon, G., Chauvaud, L., and Feng, D. (2020). Lanthanum anomalies as fingerprints of methanotrophy. *Geochem. Perspect. Lett.* 14, 26–30. doi: 10.7185/geochemlet.2019

Wang, X., Bayon, G., Kim, J.-H., Lee, D.-H., Kim, D., Guéguen, B., et al. (2019). Trace element systematics in cold seep carbonates and associated lipid compounds. *Chem. Geol.* 528, 119227. doi: 10.1016/j.chemgeo.2019.119277

Wang, X., Guan, H., Qiu, J.-W., Xu, T., Peckmann, J., Chen, D., et al. (2022). Macro-ecology of cold seeps in the south China Sea. *Geosyst. Geoenviron.* 1, 100081. doi: 10.1016/j.geogeo.2022.100081

Wang, X., Li, N., Feng, D., Hu, Y., Bayon, G., Liang, Q., et al. (2018). Using chemical compositions of sediments to constrain methane seepage dynamics: A case study from haima cold seeps of the south China Sea. *J. Asian Earth Sci.* 168, 137–144. doi: 10.1016/j.jseaes.2018.11.011

Wang, X., Li, C., and Zhou, L. (2017). Metal concentrations in the mussel bathymodiolus platifrons from a cold seep in the south China Sea. *Deep-Sea Res. Part I-Oceanogr. Res. Pap.* 129, 80–88. doi: 10.1016/j.dsr.2017.10.004

Wang, S., Wu, S., Du, M., Yang, C., and Wang, X. (2020). A new serial sampler for collecting gas-tight samples from seafloor cold seeps and hydrothermal vents. *Deep-Sea Res. Part I-Oceanogr. Res. Pap.* 161, 103282. doi: 10.1016/j.dsr.2020.103282

Wisshak, M., Neumann, C., Jakobsen, J., and Freiwald, A. (2009). The 'living-fossil community' of the cyrtocrinid cyathidium foresti and the deep-sea oyster neopycnodonte zibrowii (Azores archipelago). *Palaeogeogr. Palaeoclimatol. Palaeoecol.* 271, 77–83. doi: 10.1016/j.palaeo.2008.09.015

Wu, W., Wei, G., Xie, L., and Liu, Y. (2014). Variations of Sr/Ca, Mg/Ca ratios in seawater of the sanya bay and response of coral trace element thermometer. *Mar. Sci.* 38, 46–55. doi: 10.11759/hykx20120706003